Fluorescent Nucleosides

DOI: 10.1002/anie.201307064

Enzymatic Interconversion of Isomorphic Fluorescent Nucleosides: Adenosine Deaminase Transforms an Adenosine Analogue into an Inosine Analogue**

*Renatus W. Sinkeldam, Lisa S. McCoy, Dongwon Shin, and Yitzhak Tor**

The lack of practically useful emission for the native nucleosides A, C, G, and U(T)[1] prompted the development of fluorescent nucleoside surrogates.[2] Such emissive analogues, in conjunction with versatile and sensitive fluorescence spectroscopy techniques,[3] have shown to be of great value in the biophysical study of nucleic acids. Among the various classes of fluorescent nucleosides there are the isomorphic fluorescent nucleosides, characterized by an astute electronic and structural resemblance to the native nucleosides.[2f,4] Incorporation of such fluorescent probes is typically associated with minimal pairing, stacking, and higher structural perturbation.[2f,4] While of great value within the context of oligomeric structures and their biophysical applications, much less is known about the function of such emissive analogues in the "protein world", where nucleosides and nucleotides intricately interact with enzymes.[5]

In contrast to the use of fluorogenic enzyme substrates and fluorophore precursors[6] as well as the enzymatic unmasking or uncaging of established fluorophores for biochemical assays or imaging applications,[7] no examples exist, to our knowledge, where isomorphic fluorescent nucleosides are transformed in enzymatically catalyzed reactions to form new and distinct fluorophores. This is likely due to the substrate specificity of many of the enzymes responsible for metabolizing and utilizing such key nucleoside and nucleotide cellular components.[8] Here we investigate the utility of thA (**1**), which is a new emissive adenosine analogue and a member of our fluorescent RNA alphabet,[9] for monitoring a catabolically important deamination reaction (Figure 1a) that is catalyzed by adenosine deaminase (ADA).[10] The underlying hypothesis is that owing to its similarity to its natural counterpart adenosine, thA will be transformed to thI by ADA (Figure 1b). Since thA is emissive, thI is likely to be fluorescent as well, yet their electronic differences are expected to render the two chromophores distinct. This, in principle, should allow one to monitor the progression of the deamination reaction in real time by using fluorescence spectroscopy, an impossible task with the natural nucleobases. If successful, this can provide a new method for exploring and identifying inhibitors of ADA, small molecules of clinical utility as chemotherapeutic agents.[11] Here we demonstrate the ability of ADA, which is a chief purine metabolism enzyme with both biochemical and therapeutic significance,[11] to convert thA into thI with steady-state and kinetic analysis using absorption and emission spectroscopy. We also demonstrate the utility of this sensitive transformation monitored by fluorescence spectroscopy for the real-time detection of ADA inhibitors.

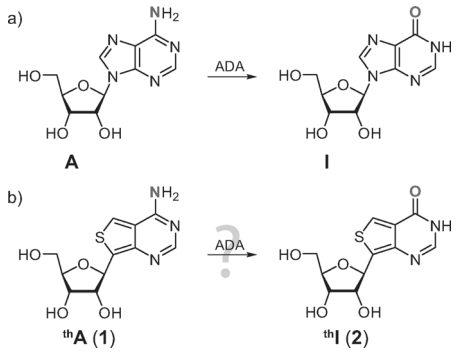

Figure 1. ADA-catalyzed interconversion of a) A to I and b) thA (**1**) to thI (**2**).

To be able to analytically and photophysically verify thI as the product of the enzymatic deamination of thA, thI was independently synthesized (Scheme 1).[9] Briefly, the syntheses of thA (**1**) and thI (**2**) started from thiophene **3**, which was reacted with β-D-ribofuranose 1-acetate 2,4,5-tribenzoate in the presence of $SnCl_4$ to give intermediate **4** as a mixture of α- and β-anomers. A subsequent tandem hydrolysis–annulation reaction furnished the protected nucleoside **5**. Following thionylation and anomer resolution, the protected nucleoside **6** was obtained as the β-anomer exclusively. A final deprotection provided thA (**1**).[9] Conveniently, deprotection of intermediate **5** followed by anomer resolution gave thI (**2**) (Scheme 1). Starting from **3**, thA (**1**) and thI (**2**) were synthesized in an overall yield of 4.6% and 10.7%, respectively. X-ray crystallography unequivocally shows their correct anomeric configuration. Overlaying their crystal structures with the reported structures of their natural counterparts A[12] and I[13] illustrates the truly isomorphic nature of thA (**1**) and thI (**2**), respectively (Figure 2 and Figure S1.1 in the Supporting Information).[14] Importantly, thA (**1**) adopts an *anti* conformation having *N*-ribose (3′-*endo*) puckering, conformational features known to be preferred by ADA.[15]

[*] Dr. R. W. Sinkeldam, L. S. McCoy, Dr. D. Shin, Prof. Dr. Y. Tor
Chemistry and Biochemistry, University of California, San Diego
9500 Gilman Drive, La Jolla, CA 92093-0358 (USA)
E-mail: ytor@ucsd.edu
Homepage: http://torgroup.ucsd.edu

[**] We thank the National Institutes of Health for support (grant GM 069773), Dr. Su, Chemistry & Biochemistry, UCSD, for help with the LC–MS experiments, and Drs. Rheingold and Moore at the X-ray facility, UCSD.

Supporting information for this article is available on the WWW under http://dx.doi.org/10.1002/anie.201307064.

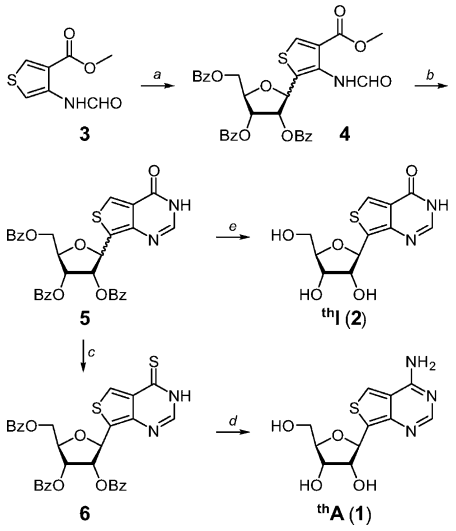

Scheme 1. Synthesis of thA (**1**) and thI (**2**). Reagents and conditions: a) β-D-ribofuranose 1-acetate 2,4,5-tribenzoate, $SnCl_4$, $MeNO_2$, 65 °C, 32%; b) 1.) 15% HCl (aq.) in MeOH, $CHCl_3$, quantitative; 2.) formamidine·AcOH, EtOH, Δ, α-anomer 21%, β-anomer 39%; c) P_2S_5, Py, 43%; d) NH_3/MeOH, 100 °C, 86%; e) NH_3/MeOH, 45 °C, 17 h (86%).

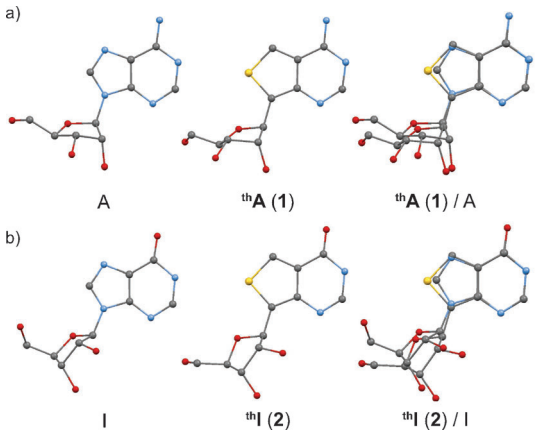

Figure 2. Crystal structures of a) A, thA (**1**), and their nucleobase overlay (RMS: 0.0383), and b) I, thI(**2**), and their nucleobase overlay (RMS: 0.0330).[14,18]

To ensure that the photophysical characteristics of thA (**1**) and thI (**2**) are distinguishable, binary mixtures containing different ratios of the two nucleosides were examined by absorption and fluorescence spectroscopy in phosphate buffer at pH 7.4; these conditions are commonly used for enzymatic deamination reactions (Figure 3a). The overlaid absorption spectra of the mixtures show a distinct hypsochromic shift of the absorption maximum from that of thA (**1**) at 339 nm to that of thI (**2**) at 315 nm with a concomitant reduction in the optical density at the lower energy transition > 300 nm (Table 1). Upon excitation at 318 nm, their isosbestic point, the recorded emission spectra also present a blue shift from 410 nm, the emission maximum of thA, to 391 nm, the emission maximum of thI. In contrast to the lower optical density, the increasing thI concentration results in an increase

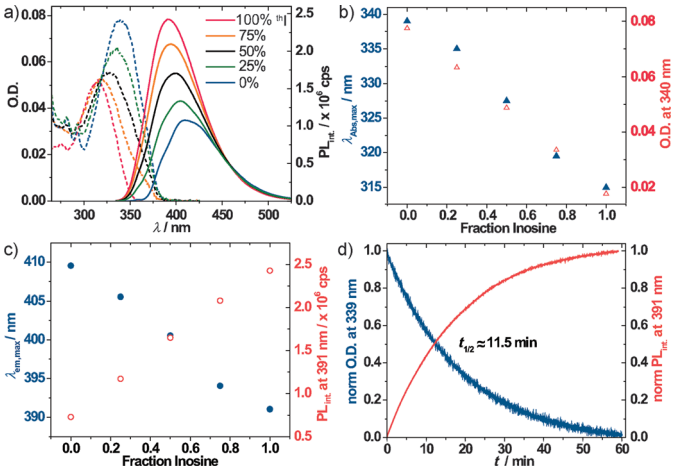

Figure 3. a) Absorption (-----) and emission (——) spectra of samples prepared with different thI/thA ratios with a total concentration of 11 μM in phosphate buffers of pH 7.4; b) correlation between inosine fraction and $\lambda_{abs,max}$ (blue ▲) and O.D. (orange △) at 340 nm; c) correlation between $\lambda_{em,max}$ (blue ●) and $PL_{int.}$ at 391 nm (orange ○); and d) enzymatic deamination of thA (**1**) to thI (**2**) with ADA monitored in real-time by absorption at 339 nm (blue) and emission at 391 nm (orange; excitation at 318 nm). Reaction conditions: [thA] = 11.7 μM, [ADA] = 27 mU mL^{-1} in phosphate buffer (50 mM, pH 7.4) kept at 25 °C for 1 h. The normalized kinetic curves yield a $t_{1/2}$ value of 11.5 min.

Table 1: Relevant spectroscopic properties of thA (**1**) and thI (**2**).

	$\lambda_{abs,max}$ [nm]	ε [M^{-1} cm^{-1}]	rel. $Abs_{int.}$ at 339 nm	$\lambda_{em,max}$ [nm]	rel. $PL_{int.}$ at 391 nm
thA (**1**)	339	7.1×10^3	3.9	410	1.0
thI (**2**)	315	4.8×10^3	1.0	391	3.3

of the emission intensity, illustrating the higher fluorescent quantum yield for thI (**2**) compared to that of thA (**1**).

To gain insight into the spectral changes, two correlation plots have been constructed (Figure 3b,c). Both the shift in absorption maximum and the drop in optical density show a nearly linear dependence on the thA/thI ratio (Figure 3b). Interestingly, both the emission wavelength and intensity respond linearly to an increasing thI concentration in binary mixtures with thA (Figure 3c). Clearly, absorption as well as emission spectroscopy reveal significant spectral changes suitable to study the enzymatic conversion of thA (**1**) to thI (**2**).

To investigate thA (**1**) as a substrate surrogate for adenosine in ADA-mediated deamination reactions, absorption and emission were measured before and after its reaction with ADA (Figure S2.2).[14] The spectra obtained after the enzymatic treatment perfectly resemble the spectral characteristics of thI (**2**; Figure 3).[14] A control experiment using a fresh solution of thI (**2**) mixed with ADA, established that the presence of the protein does not immediately affect the spectral properties of the emissive nucleoside (Figure S2.2).[14] Next, the enzymatic conversion of thA (**1**) to thI (**2**) was followed in real time using absorption as well as fluorescence spectroscopy. Absorption changes were followed at 339 nm ($\lambda_{abs,max}$ of thA), and emission changes were followed at 391 nm ($\lambda_{em,max}$ of thI) upon excitation at 318 nm, which is their

isosbestic point (Figure 3d). As expected, the absorption spectra show a decrease (or an "OFF" signal) in the optical density upon conversion of thA (**1**) to thI (**2**). By exploiting the higher fluorescence intensity of thI compared to thA to follow the enzymatic conversion, an intensification of the emission, or "ON" signal, is obtained. Absorption and emission spectra taken in the absence of ADA indicated that there is no conversion without the enzyme under the experimental conditions used.[14] LC–MS analysis unequivocally confirms the enzymatic deamination of thA (**1**) and the identity of the deamination product as thI (**2**; Figure S3.1).[14] ADA therefore recognizes thA (**1**) as a valid substrate, thereby corroborating the truly isomorphic nature of this fluorescent nucleoside analogue, and quantitatively converts it into thI (**2**) in about one hour.

The enzyme kinetic parameters V_{max} (5.15 mAbs s^{-1}) and K_m (417 μM) of the deamination reactions were determined by Henri–Michaelis–Menten analysis for both thA and A (Figure 4a,b, Table 2). The experimental results are alternatively plotted in a Lineweaver–Burk graph (Figure 4c,d, Table 2). According to the Henri–Michaelis–Menten kinetics, K_m values of 417 and 29 μM are obtained for the thA-to-thI, and A-to-I conversion, respectively. The lower conversion rate of thA, compared to that of adenosine, appears to be due to the lower affinity of the former to ADA. We speculate that the higher K_m values observed for thA are likely due to the replacement of N^7 in adenosine with a CH group in thA, as previous structural analysis has shown contacts between side chain residues and this heterocyclic position of the substrate.[10,16] Nonetheless, as demonstrated below, the performance of thA as a substrate surrogate and the enhanced and distinct emission observed upon its ADA-mediated deamination to thI, provide a robust foundation for a high-throughput assay for inhibitor discovery.

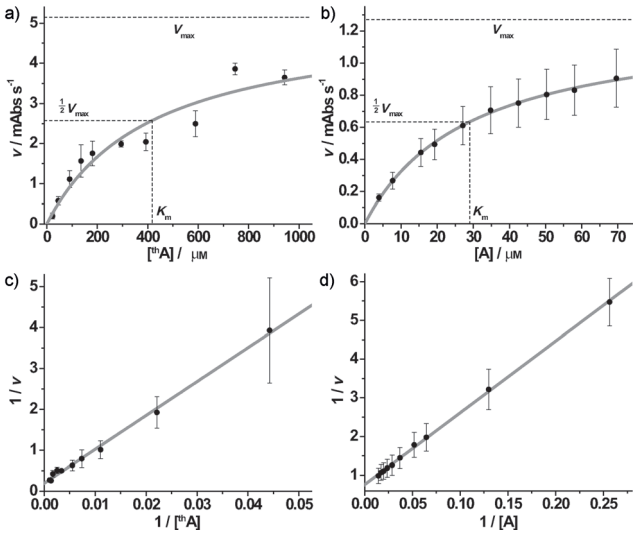

Figure 4. Henri–Michaelis–Menten plots for conversion of a) thA to thI and b) A to I. Lineweaver–Burk representations are given for conversion of c) thA to thI and d) A to I. The experiments are performed in triplicate and averaged (●). The error bars reflect the standard error of mean. For (a) and (b) the data points are fit to a Hill equation and for panel (c) and (d) the data points are linearized (gray lines). Conditions for (a,c): [thA] = 22.6–942.6 μM, [ADA] = 43.4 mU mL^{-1}, and (b,d): [A] = 3.9–69.6 μM, [ADA] = 4.1 mU mL^{-1}. All experiments are performed in phosphate buffer (50 mM, pH 7.4) at 25 °C.

Table 2: Enzyme parameters for the deamination of thA (**1**) and adenosine.

	Henri–Michaelis–Menten			Lineweaver–Burk		
	v_{max} [mAbs s^{-1}]	K_m [μM]	R^2	v_{max} [mAbs s^{-1}]	K_m [μM]	R^2
thA to thI	5.15	417	0.91247	5.07	420	0.99530
A to I	13.4[a]	29	0.99832	14.0[a]	24	0.99924

[a] The V_{max} is linearly dependent on [ADA]. To correct for the 10.58-fold lower [ADA] used in the A-to-I experiment, the apparent V_{max} (1.27 and 1.32 mAbs s^{-1}), obtained from Figure 4b and d, respectively, is multiplied by 10.58.

To illustrate the prospective for high-throughput screening and discovery of novel ADA inhibitors, which are of particular importance for the treatment of certain leukemias,[11] we developed a 96-well plate based assay, exploiting the rapid and sensitive fluorescence monitoring of the deamination reaction. The emission enhancement associated with the conversion of thA (**1**) to thI (**2**) was monitored over 60 minutes with increasing concentrations of EHNA and pentostatin, which are known ADA inhibitors (Figure 5a). The inhibition of ADA is readily apparent even at low nM concentrations (Figure 5b,c). Guanosine, used as a negative control, had no impact on the deamination reaction up to 100 nM (Figure S5.1).[14] Despite the relatively rudimentary nature of this high-throughput format, the data obtained can be easily quantified. Plotting the percent inhibition at 60 min against log[inhibitor] and applying a sigmoidal fit, yield IC_{50} values of (13.4 ± 1.3) nM and (1.9 ± 0.1) nM for EHNA and pentostatin, respectively, thereby illustrating the established higher potency of the latter (Figure 5d). We note that current methods for identifying inhibitors typically rely on either absorption spectroscopy (where other nucleoside-based inhibitory motifs are likely to cause interference) or chromatographic methods, which require relatively large quantities and are not normally amenable for high-throughput formats.

To summarize, we have demonstrated the ability of an isomorphic emissive adenosine analogue thA (**1**) to serve as a viable substrate for ADA, a nucleoside-modifying enzyme.[17] The enzymatic deamination process yields the corresponding emissive inosine analogue thI (**2**), which possesses distinct spectral features, allowing one to monitor the enzyme-catalyzed reaction and its inhibition in real time. To demonstrate its practical utility, we applied this process for the fabrication of a high-throughput assay for the discovery and biophysical evaluation of ADA inhibitors, which are key agents for researchers and clinicians. This unique proof-of-principle process, where the nucleobase core of a fluorescent nucleoside analogue is enzymatically transformed into a distinctly emissive product, demonstrates a new facet for isomorphic nucleoside analogues and expands their utility landscape beyond their "natural" and typically explored oligonucleotide environments.

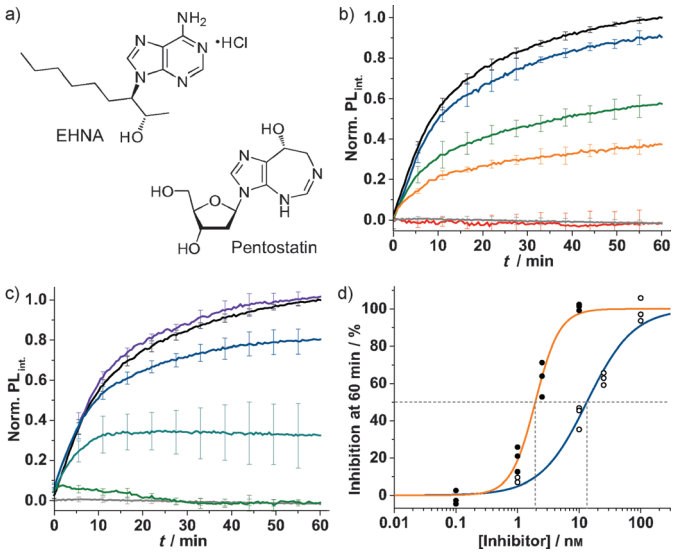

Figure 5. a) Structures of ADA inhibitors EHNA and pentostatin; b, c) conversion of thA (**1**) followed with fluorescence spectroscopy in the presence of EHNA (b; black, blue, green, orange, red lines represent [inhibitor] = 0, 1, 10, 25, 100 nM, respectively) and pentostatin (c; black, purple, blue, cyan, green lines represent [inhibitor] = 0, 0.1, 1, 2.5, 10 nM, respectively. The gray lines represent the conversion of thA (**1**) in the absence of ADA. The experiment is performed in triplicate and error bars reflect the standard deviation. d) A semi-log plot of inhibition in % at 60 min versus [inhibitor] in triplicate (data points) and sigmoidal logistic fits performed in OriginPro (lines) for EHNA (○, blue line, R^2:0.97155) and pentostatin (●, orange line, R^2:0.98437). The gray dashed lines visualize graphical determination of the IC_{50} values. Actual values have been interpolated using the fit. Assay conditions: [thA] = 11.7 μM, [ADA] = 27 mU mL^{-1}, in phosphate buffer (50 mM, pH 7.4) at 21 °C.

Received: August 11, 2013
Revised: October 6, 2013
Published online: November 29, 2013

Keywords: adenosine deamination · fluorescence · high-throughput screening · kinetics · nucleosides

[1] a) C. A. Sprecher, W. C. Johnson, *Biopolymers* **1977**, *16*, 2243–2264; b) P. R. Callis, *Annu. Rev. Phys. Chem.* **1983**, *34*, 329–357; c) J. Peon, A. H. Zewail, *Chem. Phys. Lett.* **2001**, *348*, 255–262; d) D. Onidas, D. Markovitsi, S. Marguet, A. Sharonov, T. Gustavsson, *J. Phys. Chem. B* **2002**, *106*, 11367–11374; e) B. Cohen, C. E. Crespo-Hernandez, B. Kohler, *Faraday Discuss.* **2004**, *127*, 137–147.

[2] Selected reviews: a) M. E. Hawkins, L. Brand, M. L. Johnson, *Methods Enzymol.* **2008**, *450*, 201–231; b) D. W. Dodd, R. H. E. Hudson, *Mini-Rev. Org. Chem.* **2009**, *6*, 378–391; c) Y. Tor, *Pure Appl. Chem.* **2009**, *81*, 263–272; d) L. M. Wilhelmsson, *Q. Rev. Biophys.* **2010**, *43*, 159–183; e) M. Kimoto, R. S. I. Cox, I. Hirao, *Expert Rev. Mol. Diagn.* **2011**, *11*, 321–331; f) R. W. Sinkeldam, N. J. Greco, Y. Tor, *Chem. Rev.* **2010**, *110*, 2579–2619.

[3] a) J. R. Lakowicz, *Principles of fluorescence spectroscopy*, 3rd ed., Springer, New York, **2006**; b) B. Valeur, *Molecular fluorescence, principles and applications*, Wiley-VCH, Weinheim, **2002**.

[4] Selected contributions: a) D. C. Ward, E. Reich, L. Stryer, *J. Biol. Chem.* **1969**, *244*, 1228–1237; b) N. J. Greco, Y. Tor, *J. Am. Chem. Soc.* **2005**, *127*, 10784–10785; c) C. H. Liu, C. T. Martin, *J. Mol. Biol.* **2001**, *308*, 465–475; d) Y. Tor, S. Del Valle, D. Jaramillo, S. G. Srivatsan, A. Rios, H. Weizman, *Tetrahedron* **2007**, *63*, 3608–3614; e) S. G. Srivatsan, N. J. Greco, Y. Tor, *Angew. Chem.* **2008**, *120*, 6763–6767; *Angew. Chem. Int. Ed.* **2008**, *47*, 6661–6665; f) N. B. Gaied, N. Glasser, N. Ramalanjaona, H. Beltz, P. Wolff, R. Marquet, A. Burger, Y. Mely, *Nucleic Acids Res.* **2005**, *33*, 1031–1039; g) A. Nadler, J. Strohmeier, U. Diederichsen, *Angew. Chem.* **2011**, *123*, 5504–5508; *Angew. Chem. Int. Ed.* **2011**, *50*, 5392–5396; h) Y. Xie, T. Maxson, Y. Tor, *J. Am. Chem. Soc.* **2010**, *132*, 11896–11897; i) Y. Xie, A. V. Dix, Y. Tor, *Chem. Commun.* **2010**, *46*, 5542–5544.

[5] a) V. R. Caiolfa, D. Gill, A. H. Parola, *Biophys. Chem.* **1998**, *70*, 41–56; b) V. R. Caiolfa, D. Gill, A. H. Parola, *FEBS Lett.* **1990**, *260*, 19–22; c) J. A. Secrist, J. R. Barrio, N. J. Leonard, *Science* **1972**, *175*, 646–647; d) J. A. Secrist, G. Weber, N. J. Leonard, J. R. Barrio, *Biochemistry* **1972**, *11*, 3499–3506.

[6] a) R. Haugland, I. Johnson, *J. Fluoresc.* **1993**, *3*, 119–127; b) L. D. Lavis, R. T. Raines, *ACS Chem. Biol.* **2008**, *3*, 142–155; c) L. M. Wysocki, L. D. Lavis, *Curr. Opin. Chem. Biol.* **2011**, *15*, 752–759; d) J. P. Goddard, J. L. Reymond, *Curr. Opin. Biotechnol.* **2004**, *15*, 314–322; e) J.-L. Reymond, V. S. Fluxa, N. Maillard, *Chem. Commun.* **2009**, 34–46; f) A. Rajapakse, C. Linder, R. D. Morrison, U. Sarkar, N. D. Leigh, C. L. Barnes, J. S. Daniels, K. S. Gates, *Chem. Res. Toxicol.* **2013**, *26*, 555–563; g) A. Razgulin, N. Ma, J. Rao, *Chem. Soc. Rev.* **2011**, *40*, 4186–4216.

[7] a) S. R. Adams, R. Y. Tsien, *Annu. Rev. Physiol.* **1993**, *55*, 755–784; b) T. J. Mitchison, K. E. Sawin, J. A. Theriot, K. Gee, A. Mallavarapu, *Methods Enzymol.* **1998**, *291*, 63–78; c) A. Specht, F. Bolze, Z. Omran, J.-F. Nicoud, M. Goeldner, *HFSP J.* **2009**, *3*, 255–264; d) W.-H. Li, G. Zheng, *Photochem. Photobiol. Sci.* **2012**, *11*, 460–471; e) H.-M. Lee, D. R. Larson, D. S. Lawrence, *ACS Chem. Biol.* **2009**, *4*, 409–427.

[8] a) S. Frederik, *Arch. Biochem. Biophys.* **1966**, *113*, 383–388; b) H. P. Baer, G. I. Drummond, J. Gillis, *Arch. Biochem. Biophys.* **1968**, *123*, 172–178; c) L. N. Simon, R. J. Bauer, R. L. Tolman, R. K. Robins, *Biochemistry* **1970**, *9*, 573–577; d) I. Gillerman, B. Fischer, *J. Med. Chem.* **2011**, *54*, 107–121; e) H. Follmann, H. P. C. Hogenkamp, *Biochemistry* **1971**, *10*, 186–192; f) H. Follmann in *Nuclear Magnetic Resonance Spectroscopy in Molecular Biology* (Ed.: B. Pullman), D. Reidel Publishing Company, Dordrecht, **1978**, pp. 323–337; g) N. J. Leonard, *Crit. Rev. Biochem. Mol. Biol.* **1984**, *15*, 125–199; h) D. Reinecke, F. Schwede, H.-G. Genieser, R. Seifert, *Plos One* **2013**, *8*, e54158.

[9] D. Shin, R. W. Sinkeldam, Y. Tor, *J. Am. Chem. Soc.* **2011**, *133*, 14912–14915.

[10] a) D. K. Wilson, F. B. Rudolph, F. A. Quiocho, *Science* **1991**, *252*, 1278–1284; b) T. Kinoshita, I. Nakanishi, T. Terasaka, M. Kuno, N. Seki, M. Warizaya, H. Matsumura, T. Inoue, K. Takano, H. Adachi, Y. Mori, T. Fujii, *Biochemistry* **2005**, *44*, 10562–10569; c) T. Kinoshita, N. Nishio, I. Nakanishi, A. Sato, T. Fujii, *Acta Crystallogr. Sect. D* **2003**, *59*, 299–303.

[11] a) G. Cristalli, S. Costanzi, C. Lambertucci, G. Lupidi, S. Vittori, R. Volpini, E. Camaioni, *Med. Res. Rev.* **2001**, *21*, 105–128; b) R. I. Glazer, *Cancer Chemother. Pharmacol.* **1980**, *4*, 227–235; c) P. J. O'Dwyer, B. Wagner, B. Leylandjones, R. E. Wittes, B. D. Cheson, D. F. Hoth, *Ann. Intern. Med.* **1988**, *108*, 733–743.

[12] T. F. Lai, R. E. Marsh, *Acta Crystallogr. Sect. B* **1972**, *28*, 1982–1989.

[13] U. Thewalt, C. E. Bugg, R. E. Marsh, *Acta Crystallogr. Sect. B* **1970**, *26*, 1089–1101.

[14] See the Supporting Information for additional details.

[15] H. Ford, F. Dai, L. Mu, M. A. Siddiqui, M. C. Nicklaus, L. Anderson, V. E. Marquez, J. J. Barchi, *Biochemistry* **2000**, *39*, 2581–2592.

[16] M. Ikehara, T. Fukui, *Biochim. Biophys. Acta Gen. Subj.* **1974**, *338*, 512–519.

[17] See: a) B. L. Bass, *Annu. Rev. Biochem.* **2002**, *71*, 817 – 846; b) L. Valente, K. Nishikura, *Prog. Nucleic Acid Res. Mol. Biol.* **2005**, *45*, 299 – 338; c) S. Maas, Y. Kawahara, K. M. Tamburro, K. Nishikura, *RNA Biol.* **2006**, *3*, 1 – 9; d) O. Maydanovych, P. A. Beal, *Chem. Rev.* **2006**, *106*, 3397 – 3411; e) P. Barraud, F. H.-T. Allain, *Curr. Top. Microbiol. Immunol.* **2012**, *353*, 35 – 60, for reviews of A-to-I deamination in oligonucleotides (RNA editing), a process mediated by distinct enzymes known as ADARs.

[18] CCDC-854884 (**1**) and 969749 (**2**) contain the supplementary crystallographic data for this paper. These data can be obtained free of charge from The Cambridge Crystallographic Data Centre via www.ccdc.cam.ac.uk/data_request/cif.

